11th International Symposium on Turbulence and Shear Flow Phenomena (TSFP11)
Southampton, UK, July 30 to August 2, 2019

THE SIGNATURES OF SELF-SIMILAR AND SELF-SUSTAINING PROCESSES IN THE INERTIAL REGION OF WALL TURBULENCE

Beverley J. McKeon
Graduate Aerospace Laboratories
California Institute of Technology
Pasadena, CA 91125, U.S.A.
mckeon@caltech.edu

ABSTRACT

There has been much recent progress with regards to characterizing self-similar behavior in wall turbulence in experiments, simulation, and in the mean and instantaneous forms of the Navier-Stokes equations. This paper considers some commonalities and differences between these observations, and in particular addresses the inconsistency between the attached eddy hypothesis (AEH) and self-similar scaling of the resolvent operator governing the linear dynamics of the Navier-Stokes equations. Low-rank representations of the velocity field from resolvent analysis are exploited to investigate self-similar and self-sustaining processes in wall turbulence, their signatures and limitations in physical and spectral space.

INTRODUCTION

The seminal distance-from-the-wall scaling proposed by Townsend (1951) has underpinned many theoretical and observational descriptions of wall turbulence. The original argument posits that eddies with diameters proportional to distance from the wall should be required in order to obtain a dissipation length-scale also proportional to this distance in the equilibrium (or inertial) layer, such that the motion of "the main eddies of the flow... is directly influenced by its presence" (Townsend, 1976), resulting with distance from the wall scaling for the eddy structure in all spatial directions.

These ideas have been elaborated effectively over several years into the attached eddy model (AEM), most recently reviewed in Marusic & Monty (2019), which deploys a (static, linear) superposition of hierarchies of self-similar eddies. In a discrete representation, the wall-normal eddy lengthscales (heights), $\delta_{E,m}$, are related by a geometric progression and the structures are randomly distributed over wall-parallel planes with the number of structures belonging to hierarchy m described by $N_m \sim y_m^{-2}$. Knowledge of the precise self-similar eddy form is not required to recover logarithmic scaling for the mean velocity profile and wall-parallel fluctuation variances and a constant v-variance, but is important for precise matching of higher order statistics. Recent work de Silva *et al.* (2016) has shown that including a spatial exclusion condition to prevent eddies of the same hierarchy overlapping each other leads to improved capture of higher-order statistics. Perry & Marusic (1995) noted that a wall-normal extent which scales with distance from the wall can be obtained by two types of eddies: those which reach down to the wall, i.e. $\delta_{E,m} = y_m$, as well as those which do not, $\delta_{E,mm} < y_i$, which they denoted as Type-A and Type-B eddies, respectively. The inclusion of Type-B eddies improved the accuracy of the AEM in the wake region of the flow. Information on the eddy dynamics is not immediately available (but could be determined using the Biot-Savart calculations). The predictive capabilities of the attached eddy model are rightly celebrated, and the subject of significant current study.

Flores & Jiménez (2010) and Hwang & Bengana (2016) have identified self-sustaining turbulent solutions to the Navier-Stokes equations in channel flow simulations with domains restricted to be proportional to distance from the wall, while recent work by Yang *et al.* (2019) identifies families of attached exact coherent structures. The statistics of these flows are consistent with the properties of attached eddies, and thus appear to provide evidence that the latter are multi-scale and self-sustaining within the minimal unit construction introduced by Jiménez & Moin (1991). Further, these studies give information on the dynamics of such flows, which strongly resemble those of the near-wall cycle identified in the original study. The mean momentum balance analysis (MMB) of Klewicki *et al.* , e.g. Klewicki *et al.* (2014), identifies self-similar scaling layers contributing to the mean Reynolds stress and therefore the mean velocity profile.

Here we explore the signature of self-similar and self-sustaining dynamics derived from the Navier-Stokes equations.

APPROACH

The resolvent formulation for wall turbulence has been described in detail in previous publications, e.g. McKeon and Sharma (2010) and McKeon (2017). The essential outline of the closed-loop resolvent analysis is shown in Figure 1, and the development here is for turbulent channel (plane Poiseuille) flow in a domain which is periodic in the streamwise and spanwise directions, x and z, respectively, with no-slip and no-penetration wall boundary conditions. Fourier transforming the Navier-Stokes equations in (x,z,t) and defining fluctuations relative to the spatio-temporal turbulent mean (which is assumed to be known from, e.g., experimental data, simulations or an eddy viscosity model), $\mathbf{U}(x,y,z,t) = \overline{U}(y) + \mathbf{u}(x,y,z,t)$, rearranging, and formulating in velocity-vorticity form, (v,η), we arrive at

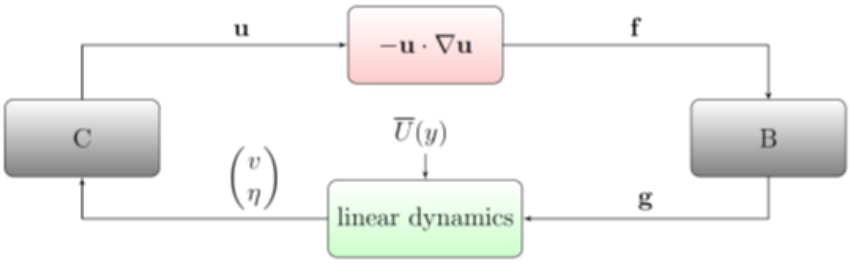

Figure 1. Cartoon of the closed loop resolvent analysis in velocity-vorticity formulation.

$$\begin{pmatrix} \hat{v} \\ \hat{\eta} \end{pmatrix} = \mathscr{H}_{\mathbf{k}} \begin{pmatrix} \hat{g}_v \\ \hat{g}_\eta \end{pmatrix} = \begin{pmatrix} \mathscr{H}_{vv} & 0 \\ \mathscr{H}_{\eta v} & \mathscr{H}_{\eta\eta} \end{pmatrix} \begin{pmatrix} \hat{g}_v \\ \hat{g}_\eta \end{pmatrix} \tag{1}$$

where

$$\mathscr{H}_{vv} = (-i\omega + k^2 = \mathscr{D}^2)^{-1} \mathscr{L}_{OS})^{-1} \tag{2}$$
$$\mathscr{H}_{\eta\eta} = (-i\omega + \mathscr{L}_{SQ})^{-1} \tag{3}$$
$$\mathscr{H}_{\eta v} = -ik_z \mathscr{H}_{\eta\eta} U' \mathscr{H}_{vv} \tag{4}$$

and $\mathscr{L}_{OS}$ is the Orr-Sommerfeld operator. Here $\hat{g}_v$ and $\hat{g}_\eta$ represent the nonlinear forcing of the linear velocity/vorticity terms at $\mathbf{k} = (k_x, k_z, \omega)$ arising from the linear interactions between other scales, and the $\mathscr{H}$ constituting the resolvent (transfer function) are related to the well-known Orr-Sommerfield and Squire operators.

The velocity components are recovered via

$$\begin{pmatrix} \hat{u} \\ \hat{v} \\ \hat{w} \end{pmatrix} = C \begin{pmatrix} \hat{v} \\ \hat{\eta} \end{pmatrix} \tag{5}$$

and the forcing in $v-\eta$ space is given by

$$\begin{pmatrix} \hat{g_v} \\ \hat{g_\eta} \end{pmatrix} = B\hat{\mathbf{f}} = \begin{pmatrix} \hat{f_u} \\ \hat{f_v} \\ \hat{f_w} \end{pmatrix} = - < \mathbf{u}.\nabla\mathbf{u} >_{\mathbf{k}} \tag{6}$$

Input-output analysis of this form was described by Jovanovic and Bamieh (2005) for laminar flow, and several other studies have considered the characteristics of the linear resolvent operator using an eddy viscosity rather than the explicit nonlinear term to provide a closure, e.g. Hwang and Cossu (2010). A singular value decomposition (SVD) of the resolvent transfer function can be used to obtain a basis set of forcing and associated response modes ranked by gain (singular value).

Further decomposition into Orr-Sommerfield and Squire modes (Rosenberg & McKeon (2019)), forced by g_v and g_η (only), respectively, leads to an efficient basis by which to represent the full turbulent field with high fidelity; for simplicity here we consider only the singular response modes associated with the full resolvent operator, $\mathscr{H}$, from Equation 1. The appropriate weights, $\chi_j(k_x, k_z, \omega)$, for each basis function can be determined either by consideration of the nonlinear interaction of response modes at other $\mathbf{k}$ combinations or from data, as summarized in McKeon (2017).

The resolvent operator has been found to be surprisingly low-rank in the wavenumber-frequency range where turbulence is energetic (Moarref et al., 2013), such that only a low number of resolvent response modes are required to capture key physical features. This low-rank behavior is exploited here, where we employ only the first singular (forcing and response) modes to examine structure in the inertial region. Further details pertaining to the results presented here may be found in McKeon (2019).

The question to be addressed here, with reference to Figure 1 is: in what regions of the flow and under what conditions (if any) will the *full, nonlinear* loop exhibit self-similar behavior, and how does the associated structure compare with existing, known scalings?

SELF-SIMILARITY OF THE RESOLVENT AND NONLINEAR FORCING IN THE INERTIAL REGION

Considering first the linear part of Figure 1, the general conditions for self-similarity of the resolvent operator have been outlined by Hwang & Cossu (2010) and Moarref *et al.* (2013). Geometric self-similarity of the response modes is possible in the inertial region, provided the following three conditions are met: the mean velocity profile is logarithmic, the support of the modes is within the log region, and the modes have an aspect ratio such that $k_x \ll k_z$. Under these constraints, hierarchies can be defined on which the response modes are self-similar under the scalings

$$\hat{k_x} = k_x y_c y_c^+ = \alpha; \quad \hat{k_z} = k_z y_c = \beta; \quad \hat{y} = y/y_c \tag{7}$$

where α and β are constants and y_c denotes the mode critical layer, where $\overline{U}(y_c) = \omega/k_x = c$. A sketch of such hierarchies and the collapse of streamwise mode shapes on a sample hierarchy are shown in Figure 2. These scalings are consistent with the AEM in y and z, both of which scale with distance from the wall, but notably different from the AEM with regards to streamwise wavenumber.

Concerning the nonlinear forcing, Moarref *et al.* (2014*a*) and Sharma *et al.* (2016) showed that the nonlinear interaction of modes on self-similar hierarchies also exhibits self-similar behavior in the inertial region. If modes on three hierarchies at one distance from the wall are triadically consistent (resonant), then they will be so at larger y values. The mode weights are governed by

$$\chi_{m1} = \sum_{m2,m3} \mathscr{N}_{m,123} \chi_{m2} \chi_{m3} \tag{8}$$

where the interaction coefficient, $\mathscr{N}$, is self-similar, such

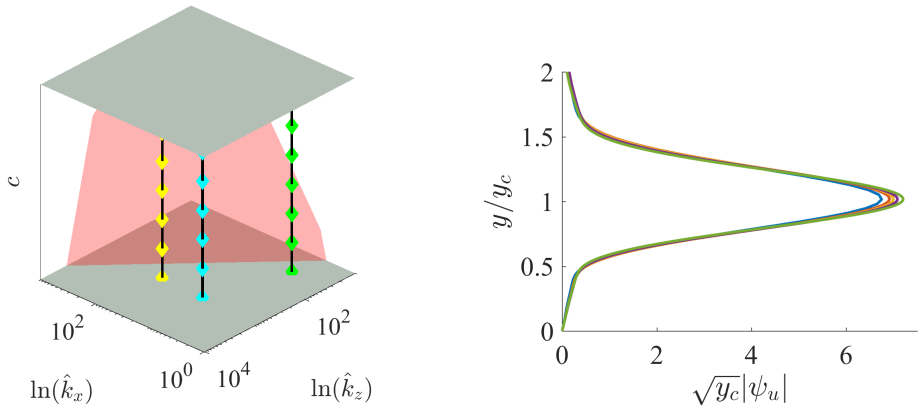

Figure 2. Left: schematic showing three self-similar hierarchies (vertical lines) and the location of $k_x = 3k_z$, shown as the red inclined plane. Below this plane the approximate streamwise-spanwise mode aspect ratio for self-similarity is not achieved. After Moarref *et al.* (2013). Right: collapse of scaled u modes on a sample hierarchy.

that at y_m and y_n:

$$\mathcal{N}_{m,123} = \int \phi^*_{m1}.(\psi_{m2}.\nabla\psi_{m3})\mathrm{d}y \tag{9}$$

$$\mathcal{N}_{n,123} = e^{-2.5\kappa(c_n - c_m)}\mathcal{N}_{m,123} \tag{10}$$

Thus for $y_n = Ay_m$, $\chi_{1n} = f(A)\chi_{1m}$.

Both the linear and nonlinear components of the resolvent framework exhibit self-similarity, and thus there exists the possible of self-sustaining assemblies of hierarchies which lead to self-similar behavior with y.

SELF-SIMILAR STRUCTURE AND SIGNATURES

While the resolvent scaling in the streamwise component deviates in a spectral sense from the AEM distance-from-the-wall scaling, the physical structure associated with members of a hierarchy represents a more faithful comparison to attached eddies as proposed by Townsend. Thus we consider the streamwise velocity signature associated with one self-similar hierarchy. The flow studied is channel flow at $Re_\tau = 15{,}000$ and the hierarchy has reference parameters $(\lambda_r, c_r) = (29, 123, U(y_{c5}))$. Discrete members of the hierarchy are obtained in the inertial region, $y^+ > 3/\sqrt{Re_\tau}$, via a geometric progression with $A = 2$, i.e. $y_{c,m+1} = y_{c,m}/2$. The (five) locations of the y_c values are marked with black dashed lines in the subsequent figures. The magnitudes of the modes are chosen to give the same peak amplitude, 10% of the channel centerline velocity (note that the surfaces of zero velocity will be only weakly dependent on the magnitudes), and the phases reflect either symmetry (Figures 3-5) or antisymmetry (Figures 6-8) around $z = 0$, for ease of visualization. Modes on a single hierarchy are not triadically consistent. Because the members of a hierarchy convect with different velocities, modes experience all phases relative to each other over time.

Figure 3 shows the variation of the composite u signal from the members of the hierarchy in a streamwise/wall-normal plane, i.e. for a fixed spanwise location, $z_0 = 0$. The chosen value of A ensures overlap of each mode with immediate neighbors in y (independent of the mode amplitude). Tracking the negative (blue) isocontours reveals the presence of extended structures which have a footprint down to the wall from each y_c. For example, the negative isocontours observed at $y_c \approx 0.4$ reach down to the wall. Negative isocontours observed at $y_c \approx 0.2$ but not at 0.4 also reach to the wall. These structures are self-similar according to the scaling of Equation 7, as shown in the zoomed-in regions from Figure 3 in Figure 4. In a field of view spanning two periods of the largest wavelength mode, one observes two structures of the tallest kind, four of the next smallest, with the smaller structures interspersed between the larger ones, etc. Thus, while self-similarity of the equations of motion (through the resolvent) requires a streamwise wavelength of $\lambda_x \sim y_c^2$ on the hierarchy, the effective spacing of structures at a given y_c is given by $\tilde{\lambda}_x = y_c^2/2 \sim y_c$, which is consistent with AEH scaling.

Figure 5 shows the sum of the same fluctuation field and the mean velocity profile (the inferences from this analysis are robust to the exact ratio of centerline velocity to mode magnitude here). Saxton-Fox & McKeon (2016) demonstrated that the summing of a response mode and the mean profile leads to an asymmetric (in y, about y_c) instantaneous velocity field because of the monotonic decay of the mean shear with distance from the wall, with "bulge" and "ramp" structures reminiscent of the coherence observed in real flows. Because the mean profile as well as the fluctuations are self-similar in the overlap region, Figure 5 reveals self-similar bulges of low momentum fluid associated with different positions on the hierarchy. These have the same space-filling distribution as described for the fluctuations of Figure 3, but these are the likely equation-driven analogs of Townsend's attached eddies, since they pertain to the instantaneous velocity rather than just the velocity fluctuation. Further, this accounting for structure rather than spectral scaling identifies the self-similarity of coherent regions and a possible explanation for hints of fractal behavior in earlier studies.

Three-dimensional isosurfaces of fluctuation are shown in Figure 6 for modes with the same y_c values as the preceding figures, but antisymmetry about $z = 0$. The sub-unit of two streamwise wavelengths and half a spanwise wavelength of the uppermost member of the hierarchy of Figure 7(a) is color-coded by the appropriate scaling height, i.e. the height of the aggregated structure, in 7(b). Associated with a single unit of the tallest structure (shown

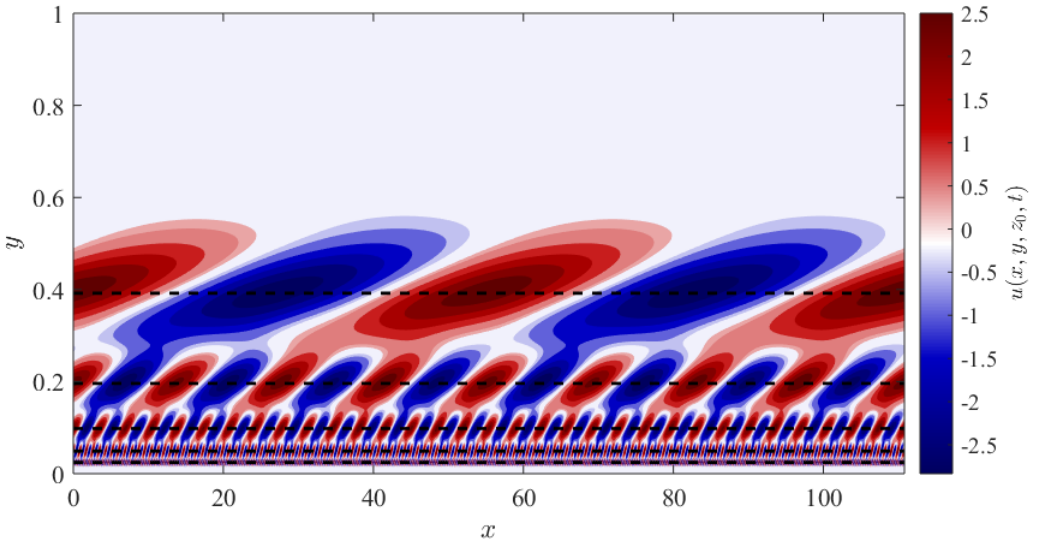

Figure 3. Snapshot of the streamwise velocity fluctuation, $u^+(x,y,z_0,t_0)$, in a streamwise/wall-normal plane obtained from a self-similar family of resolvent modes with $(\lambda_r, c_r) = (29, 123, U(y_{c5}))$ and $y_{m+1} = 2y_m$ at $Re_\tau = 15{,}000$. Lowest member of the hierarchy occurs at the start of the inertial region, $y_5 \approx 3/\sqrt{Re_\tau}$. Red and blue colors denote positive and negative values of u^+, respectively, and the x-direction is normalized with respect to the longest mode in the hierarchy which is plotted.

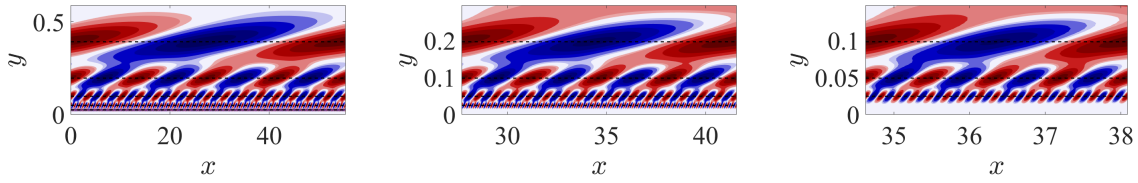

Figure 4. Snapshot of the streamwise velocity fluctuation, $u^+(x,y,z_0,t_0)$, in a streamwise/wall-normal plane obtained from the same self-similar family of resolvent modes as in Figure 3.

in green) are four structures of the next smallest scale (in blue), sixteen of the next smallest (in yellow), etc., such that the number of structures of any scale relative to the number of the largest one, N_1, is given by

$$N_m = \left(\frac{y_{c,m}}{y_{c,1}}\right)^2 N_1. \tag{11}$$

The appropriate ensuing accounting of structures at a given wall-parallel plane is shown in schematic in Figure 8.

SUMMARY

The implications of self-similarity on coherent structure in the logarithmic region and the connections between the spectral picture afforded by the resolvent analysis and the attached eddy hypothesis have been discussed. The resolvent mode representation permits investigation of the dynamics of the self-similar hierarchies, as well as the potential for self-sustenance of an assembly of such hierarchies, both of which are absent from the classical AEM. The apparent conflict between geometric self-similarity of the linear Navier-Stokes operator for turbulent flow and the full distance-from-the-wall scaling of Townsend and the AEM can be conceptually resolved by making an "apples-to-apples" structural comparison, following the common AEM representation of a geometric progression (rather than a continuous distribution) of eddy sizes. The aggregated structures associated with a geometrically self-similar resolvent hierarchy obey the attached eddy scaling; however the analogy is not complete: these aggregations exist relative to the turbulent mean profile, which is assumed (equally, acts as a constraint) in the resolvent framework.

The results of Moarref *et al.* (2014*b*) and Sharma *et al.* (2016) concerning self-similarity of the nonlinear interactions between resolvent hierarchies reveal the possibility of self-sustaining assemblies of hierarchies, with likely connection to the self-similar, self-sustaining solutions obtained in minimal unit simulations in the logarithmic layer.

The connection between the velocity response modes which are naturally most amplified in the equations of motion, parameterized in spectral space, and empirical physical space reasonings going back to Townsend seems to hold promise both for improved modeling in both domains. We have focused on the first resolvent modes herein, but the approach can be extended to consider higher rank resolvent approximations and to include the separate consideration of Orr-Sommerfield and Squire contributions to the wall-normal vorticity, which was identified by Rosenberg & McKeon (2019) as an important step in obtaining an efficient basis to represent real flows. The weights, $\chi_j(\lambda, c)$, hold the key to nonlinear closure of the resolvent framework; the work herein suggests that analytical progress to complement data-driven resolvent approaches may be made.

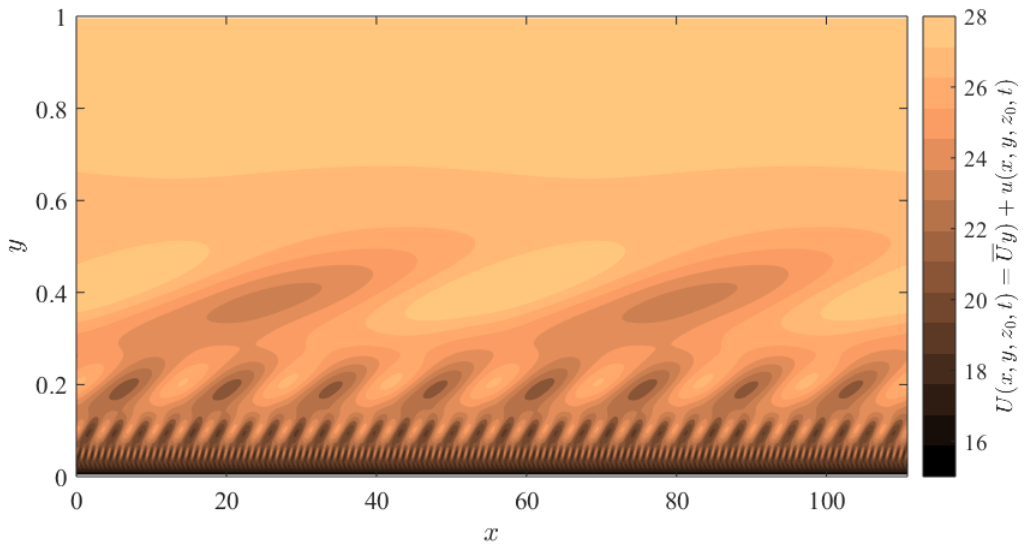

Figure 5. Snapshots of the instantaneous streamwise velocity, $U(x,y,z_0,t) = \overline{U}(y) + u(x,y,z_0,t_0)$, in a streamwise/wall-normal plane obtained from the same self-similar family of resolvent modes as in Figure 3.

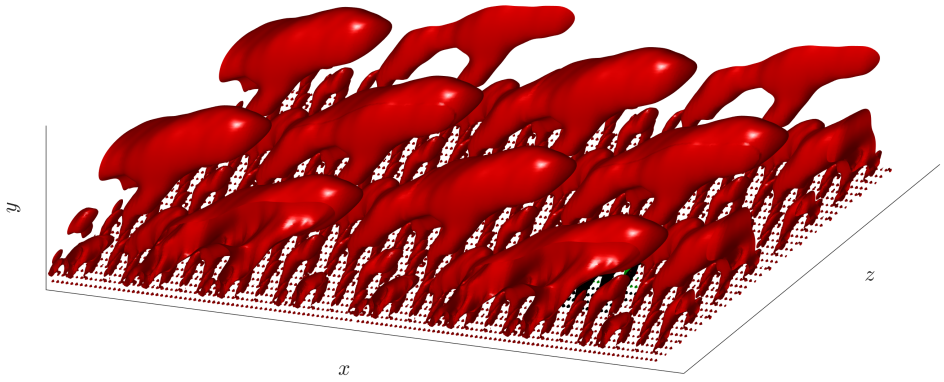

Figure 6. Three-dimensional isosurfaces of negative $U(x,y,z,t_0)$ for $z = 0$ antisymmetric modes.

Further connections with the mean momentum balance analysis, which pertains to self-similarity of a hierarchical distribution of contributions to the Reynolds stress, $\overline{-uv}$, determined from the mean momentum equation in the inertial range, and exact coherent structures in the logarithmic region, which have connections with self-similar nonlinear interactions of resolvent modes, are the subject of ongoing work.

ACKNOWLEDGEMENTS

The support of the U.S. Office of Naval Research under grant N00014-17-1-2307 is gratefully acknowledged.

REFERENCES

Flores, O. & Jiménez, J. 2010 Hierarchy of minimal flow units in the logarithmic layer. *Phys. Fluids* **22** (071704).

Hwang, Y. & Bengana, Y. 2016 Self-sustaining process of minimal attached eddies in turbulent channel flow. *J. Fluid Mech.* **795**, 708–338.

Hwang, Y. & Cossu, C. 2010 Linear non-normal energy amplification of harmonic and stochastic forcing in the turbulent channel flow. *J. Fluid Mech.* **664**, 51–73.

Jiménez, J. & Moin, P. 1991 The minimal flow unit in near-wall turbulence. *J. Fluid Mech.* **225**, 213–240.

Klewicki, J. C., Philip, J., Marusic, I., Chauhan, K. & Morrill-Winter, C. 2014 Self-similarity in the inertial region of wall turbulence. *Phys. Rev. E* **90**, 823–839.

Marusic, I. & Monty, J. P. 2019 Attached eddy model of wall turbulence. *Annu. Rev. Fluid Mech.* **51**, 49–74.

McKeon, B. J. 2017 The engine behind (wall) turbulence: perspectives on scale interactions. *J. Fluid Mech.* **817**, P1.

McKeon, B. J. 2019 Self-similar hierarchies and attached eddies. *(submitted)* .

Moarref, R., Jovanović, M. R., Sharma, A. S., Tropp, J. A.

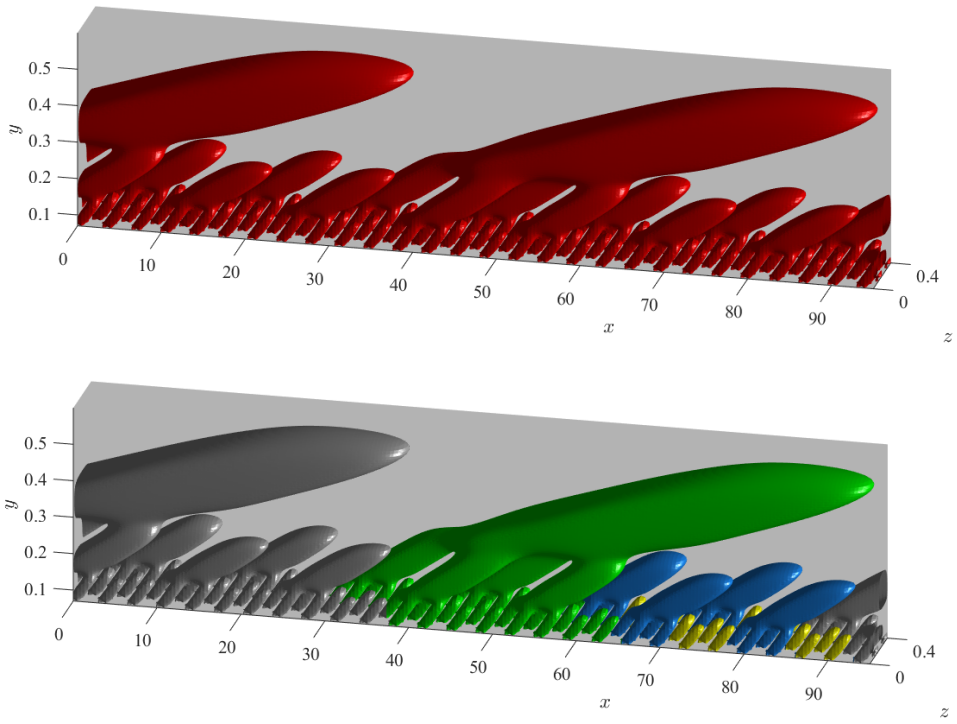

Figure 7. Top: zoomed in version of Figure 6, showing two streamwise period and a half spanwise period of the largest scale. Bottom: aggregated structures in a single period of the largest scale color-coded by the appropriate scaling height, y_{cm}. Green, blue and yellow: m=1,2,3, respectively.

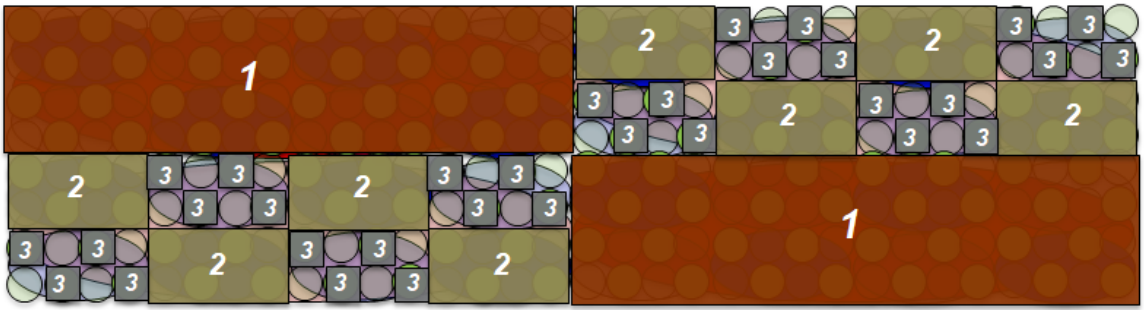

Figure 8. Schematic of the apportioning of the signature of aggregated scales on a wall-parallel plane, showing the scaling of Equation 11. Numbers denote the signature of a structure centered at y_m.

& McKeon, B. J. 2014*a* A low-order decomposition of turbulent channel flow via resolvent analysis and convex optimization. *Phys. Fluids* **26** (051701).

Moarref, R., Sharma, A. S., Tropp, J. A. & McKeon, B. J. 2013 Model-based scaling and prediction of the streamwise energy intensity in high-Reynolds number turbulent channels. *J. Fluid Mech.* **734**, 275–316.

Moarref, R., Sharma, A. S., Tropp, J. A. & McKeon, B. J. 2014*b* A foundation for analytical developments in the logarithmic region of turbulent channels. *ArXiv* (1409.6047).

Perry, A. E. & Marusic, I. 1995 A wall-wake model for the turbulence structure of boundary layers. Part 1. Extension of the attached eddy hypothesis. *J. Fluid Mech.* **298**, 361–388.

Rosenberg, K. & McKeon, B. J. 2019 Efficient representation of exact coherent states of the Navier-Stokes equations using resolvent analysis. *Fluid Dyn. Res.* **51** (011401).

Saxton-Fox, T. & McKeon, B. J. 2016 Scale interactions and 3D critical layers in wall-bounded turbulent flows. In *Proc. ICTAM*.

Sharma, A. S., Moarref, R. & McKeon, B. J. 2016 Scaling and interaction of self-similar modes in models of high-Reynolds number wall turbulence. *Phil. Trans. Royal Soc. A* **375(2089)** (20160089).

de Silva, C. M., Woodcock, J. D., Hutchins, N. & Marusic, I. 2016 Influence of spatial exclusion on the statistical behavior of attached eddies. *Phys. Rev. Fluids* **1** (022401).

Townsend, A. A. 1951 The structure of the turbulent boundary layer. *Math. Proc. Camb. Philos. Soc.* **47**, 375–395.

Townsend, A. A. 1976 *The Structure of Turbulent Shear Flow*. Cambridge, UK: Cambridge University Press.

Yang, Q., Willis, A. P. & Hwang, Y. 2019 Exact coherent states of attached eddies in channel flow. *J. Fluid Mech.* **862**, 1029–1059.